Curvelet-based ground roll removal

Carson Yarham, Urs Boeniger, Felix Herrmann, Seismic Laboratory for Imaging and Modeling at the University of British Columbia

SUMMARY

We have effectively identified and removed ground roll through a two-step process. The first step is to identify the major components of the ground roll through various methods including multiscale separation, directional or frequency filtering or by any other method that identifies the ground roll. Given this estimate for ground roll, the recorded signal is separated during the second step through a block-coordinate relaxation method that seeks the sparsest set for weighted curvelet coefficients of the ground roll and the sought-after reflectivity. The combination of these two methods allows us to separate out the ground roll signal while preserving the reflector information. Since our method is iterative, we have control of the separation process. We successfully tested our algorithm on a real data set with a complex ground roll and reflector structure.

INTRODUCTION

The removal of ground roll from seismic records forms an integral part of the signal processing flow. Land-based seismic data are commonly affected by these events that are generally considered to be noise. The low-frequency and high-amplitude characteristics of ground roll interfere with the primary reflected signals and must be removed before the data can be subjected to subsurface evaluations.

Numerous authors have been shown that the effect of ground roll can be reduced by proper acquisition design and filtering (Brown and Clapp, 2000; Harland et al., 1984; Shieh and Herrmann, 1990). Unfortunately, these methods may either fail to remove all the ground roll or may lead to unacceptable deterioration of the primary reflections. In addition, there may be geographical, financial, or logistical limitations that may dictate a less-then-optimal survey design for the reduction of noise during acquisition. Due to these reasons there is still a demand for efficient filtering techniques for ground roll removal.

In this paper, we develop a new and effective method of identifying and removing ground roll using the curvelet transform (as designed by Candès et al. (2005)). Given a possibly inaccurate first estimate for the ground roll, the data is separated through a sparsity promoting block-coordinate relaxation solver (Elad et al., 2005; Herrmann et al., 2006) that separates the signal into ground roll and reflective signals. Since this method involves two stages, this procedure can be repeated using the estimated reflectors as input. During this iterative process, the ground roll is again predicted and used as weights in the next iteration driving the two signal components apart.

During the prediction/removal process, the scale and angle separation properties of the curvelet transform are used to remove the oscillatory, fine-scale component of the ground roll. The estimate for the ground roll is obtained and then used as an input to a nonlinear separation technique in the context of primary-multiple separation Herrmann et al. (2006). This process can be repeated at lower scales but is most effective at the two highest.

After we have used these predictions to separate this component of the ground roll signal, we can create another prediction with traditional band pass filtering. Instead of removing the components directly, we separate the two signals through the block solver in the same way used to removed the previous predictions. As we will show, this separation method is robust under errors in the amplitude and phase of the predicted ground roll.

Since the separation is performed in the curvelet domain, spurious curvelet artifacts may remain and we attempt to remove these with an additional Bayesian thresholding procedure.

SEPARATION METHOD

Within each step of our iterative procedure we have two tasks to accomplish. First, we need to generate a representative ground roll prediction which allows us to cast the second task of ground roll reflectivity separation. A nonlinear optimization problem is solved for the unknown augmented vector $\mathbf{x}_0 = [\mathbf{x}_1, \mathbf{x}_2]^T$ with the two signal components, from noise corrupted data

$$\mathbf{y} = \mathbf{A}\mathbf{x}_0 \tag{1}$$

with $\mathbf{y}$ the total data including ground roll and white noise, $\mathbf{A} = \left[\mathbf{C}^T, \mathbf{C}^T\right]$ the curvelet synthesis matrix with $\mathbf{C}^T$ the inverse curvelet transform. Provided $\mathbf{x}_0$ is sparse enough, $\mathbf{x}_0$ can be recovered when we are given a first estimate for the ground roll $\check{\mathbf{s}}_2$, from which we can obtain a first estimate for the reflected data according $\check{\mathbf{s}}_1 = \mathbf{s} - \check{\mathbf{s}}_2$ with $\mathbf{s}$ as the total data. By using these estimates as weights in the following optimization problem

$$\hat{\mathbf{x}}_j = \arg\min_{\mathbf{x}_j} \frac{1}{2}||\mathbf{y} - \mathbf{A}_j\mathbf{x}_j - \sum_{i\neq j}\mathbf{A}_i\mathbf{x}_i||_2^2 + ||\mathbf{x}_j||_{1,\lambda_m\cdot\mathbf{w}_j} \qquad j = 1,\ldots,2, \tag{2}$$

an estimate for $\mathbf{x}$ is obtained. From this estimate the reflected signal and ground roll follow according $\hat{\mathbf{s}}_1 = \mathbf{C}^H\hat{\mathbf{x}}_1$ and $\hat{\mathbf{s}}_2 = \mathbf{C}^H\hat{\mathbf{x}}_2$. The weights in the above expression are set according to

$$\begin{cases} \mathbf{w}_1 := C_1|\check{\mathbf{s}}_2| \\ \mathbf{w}_2 := C_2|\check{\mathbf{s}}_1| \end{cases} \tag{3}$$

The above optimization problem forms the iterative loop of the optimization problem with the constants C_1 and C_2 controlled by the $L1$ norms of the weights and predictions. This loop repeats as long as $\varepsilon > \beta$ with $\varepsilon = \hat{\mathbf{s}} - (\hat{\mathbf{e}}s_1 + \hat{\mathbf{s}}_2)$ and β representing an acceptable separation error. By working within these conditions, we make sure that we do not throw out any meaningful data and only accept any acceptable error limit β.

Ground Roll Estimation

The curvelet transform has several properties that make it useful for generating ground roll predictions. A graphical expression of the separate scales inhabited by the ground roll and reflectivity in the Curvelet domain can be observed in Figure 2. The low linear velocity component and high-amplitude variations of ground roll combined with the sampling parameters tends to compress the waveforms horizontally in the $t-x$ domain. This compression will tend to map these components of ground roll to the finest curvelet scales. Through this property we preform a threshold on the finest scale coefficients which creates a good initial estimation of the ground roll.

After separation of the ground roll in the finest scale, we can look at how the ground roll maps to the second finest scale. In this domain we observe that ground roll is mixed in with the reflectors but since the ground roll is characterized by generally larger amplitudes, we can still define a threshold based on the curvelet amplitudes once again and

use this to define a new prediction for the ground roll that is within the second finest scale. This can be done for any scale but generally we find that this is effective for lower scales as the ground roll components do not separate from the reflector components which leads to reflector removal.

Once the textural component of the ground roll is removed the majority of the ground roll signal is contained in the low frequency components. Using a 1-D filter on the traces, we isolate this component. This can be utilized to create another estimate for the ground roll itself which we can use with the block solver to separate the signal again.

One other method that we will employ is a scale dependent Bayesian threshold. This method helps to clean up the signal of any residual noise and minor artifacts that may have been introduced through the curvelet thresholding that occurs within the block solver.

Application of block-coordinate relaxation method

Based on the methods defined by Elad et al. (2005), we have implemented a similar scheme to facilitate the separation of our two signals. The benefits of this system are two fold. First, they allow completely individual separations. It has been shown by Starck et al. (2004) that this iterative soft thresholding is equivalent to solving and ℓ_1 minimization which is how we wish to separate our signal. Secondly, the two output signals are completely separated from each other allowing for a step-wise removal scheme to be implemented. Third, we can control the error of the separation thus allowing flexibility for optimizing error versus computational cost.

To initiate separation, we must first define the separation conditions using a noise prediction which is calculated. This prediction is used to define the weighted soft thresholding which facilitates the signal separation.

The block solver works in a similar manner to that developed by Elad et al. (2005) with a few adaptations. Instead of using separate transforms, we use a single transform. Instead of relying on the sparsity of the two signals in separate domains, we use the fact that our signals are both sparse in the curvelet domain and then weight them appropriately. The signal is separated into two estimations based on the prediction weights. While one estimation is fixed, the estimation of the second is updated by solving the block solver with a weighted threshold. Following that the second prediction is fixed and the first updated. This continues while λ is reduced after ever pair to facilitate a cooling method based on Elad et al. (2005). This method drives the two signals apart iteratively leaving us with our calculated noise based on our estimate and our predicted reflector signals.

Bayesian Threshold

As a final processing step we apply a Bayesian Threshold to our data set. This is an optional step that has shown promising results with some draw backs. This thresholding method has been derived from Krishnaveni et al. (2004) and is defined as

$$\delta(x) = \begin{cases} 0 & |x| \leq \alpha \\ x & |x| > \alpha, \end{cases} \quad with \quad \alpha = \Psi \sqrt{\frac{1}{N} \sum_{i=1}^{N} (x_i - \bar{x})^2} \qquad (4)$$

as the standard deviation for each individual curvelet scale. This threshold can be utilized to remove some of the artifacts produced by thresholding in the curvelet domain. As we will see, there is work to be done regarding this technique as it does have a tendency to effect the reflector signal but by optimizing the constant Ψ this should be able to be improved.

NUMERICAL RESULTS

The dataset that we decided to use for testing the efficiency of our denoising scheme is referred to as the Oz 25 dataset (Figure 1). We have chosen this dataset due to a few factors, first being the large amount of ground roll that dominates this dataset. We can see that the entire center of the dataset is covered in this coherent noise. Another reason that we have chosen this dataset is due to the variable reflectivity of the reflectors. By having reflector signals that range from thin weak layers near the top to more promonant layers in the center allows us to judge the effect of our technique on a wide range of these returns. This is critical as we want to preserve the reflector information while removing the ground roll signal.

After selection of our ground roll predictions through methods of selective scale reconstruction and low frequency predictions we can reconstruct our separated data represented in figure 3(a). Our residual image or calculated noise is shown in figure 3(b). We can see that we have effectively separated the two signal components into ground roll and reflectors. Looking specifically at figure 3(b) we can see that there almost no cross contamination of the reflector signal. This shows that the reflectors have been almost entirely preserved with no major effects.

For an enlarged view of the results we can look at figures 5(a), 5(b) and 5(c). We can see from this view that there has been significant improvement of the signal with regards to the ground roll removal. Again, in figure 5(c) we see minimal signs of reflector removal from our dataset.

Lastly, the Bayesian thresholding results are shown in figures 4(a) and 4(b). The imaging of the reflector signals has been improved through this method of artifact removal but as we can see in the differences between figures 3(b) and 4(b) that there has been a small amount of reflector removal. This may be reduced by adjusting the constant values in the threshold. Artifact suppression and minimization is a current area of interest and research and is ongoing.

FIGURES

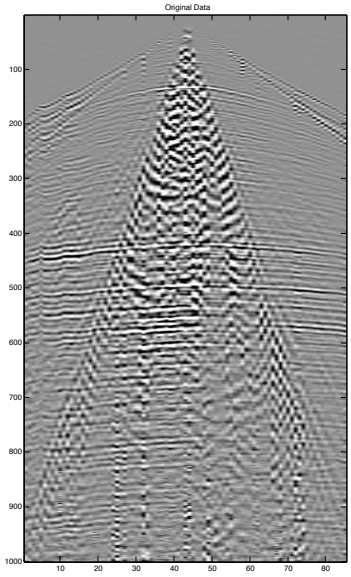

Figure 1: Oz 25 dataset.

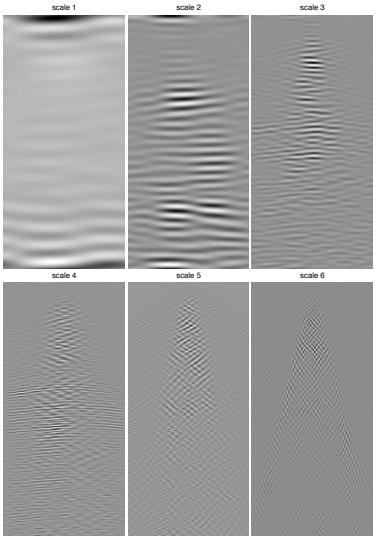

Figure 2: Separate scale reconstructions of the Oz 25 dataset.

ACKNOWLEDGMENTS

The authors would like to thank the authors of the Fast Discrete Curvelet Transform (FDCT) for making this code available at www.curvelets.org. This work was in part financially supported by NSERC Discovery Grant 22R81254 of Felix J. Herrman and was carried out as part of the SINBAD project with support, secured through the Industry Technology Facilitators from the following orginazations: BG Group, BP, Chevron, ExxonMobil and Shell.

REFERENCES

Brown, M. and Clapp, R. G., 2000, (t,x) domain, pattern-based ground roll removal.

Candès, E., Donoho, D., Demanet, D., and Ying, L., 2005, Fast discrete curvelet transforms.

Elad, M., Starck, J. L., Querre, P., and Donoho, D., 2005, Simultaneous cartoon and texture image inpainting using morphological component analysis (mca): Journal on Applied and Computational Harmonic Analysis, **19**, 340–358.

Harland, W., Claerbout, J., and Rocca, F., 1984, Signal/noise separation and velocity estimation: Geophysics, **49**, 1869–1880.

Herrmann, F., Boeniger, U., and Verschuur, D., 2006, Nonlinear primary-multiple separation with directional curvelet frames. (Submitted).

Krishnaveni, V., Jayaraman, S., Malmurugan, N., Kandaswamy, A., and Ramadoss, K., 2004, Non adaptive thresholding methods for correcting ocular artifacts in eeg: Academic Open Internet Journal, **13**.

Shieh, C. and Herrmann, R. B., 1990, Ground roll: Rejection using polarization filters: Geophysics, **55**.

Starck, J. L., Elad, M., and Donoho, D., 2004, Redundant multiscale transforms and their applications to morphological component separation.: Advances in Imaging and Electron Physics, **132**.

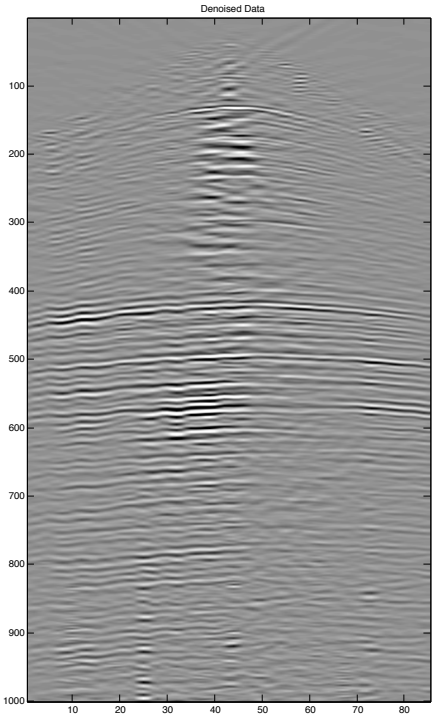

(a)

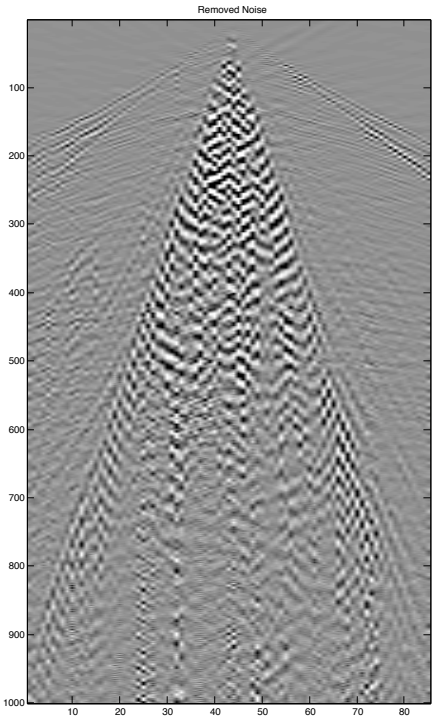

(b)

Figure 3: The denoised Oz 25 dataset with the residual noise. We can see by looking at the residual noise that there is very little reflector signal removal.

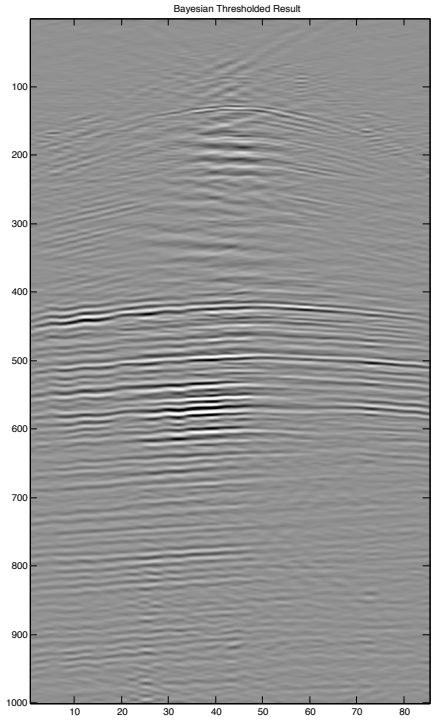

(a)

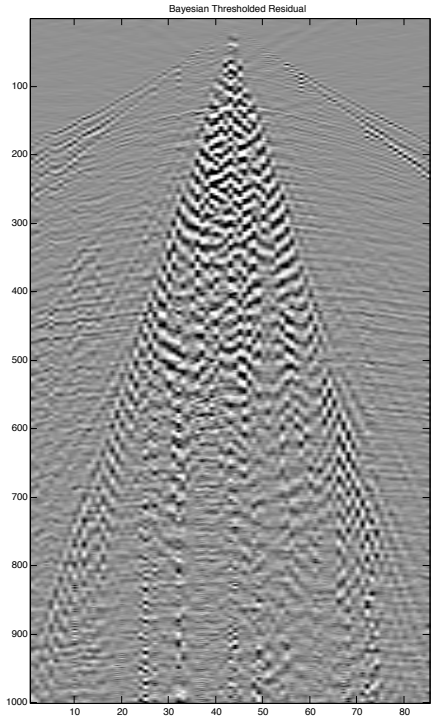

(b)

Figure 4: The denoised Oz 25 dataset with the residual noise after application of the bayesian threshold. By comparing the residual noise images between the two results we can see that there is a slight increase in reflector removal with this method but the denoised result also contains less clutter.

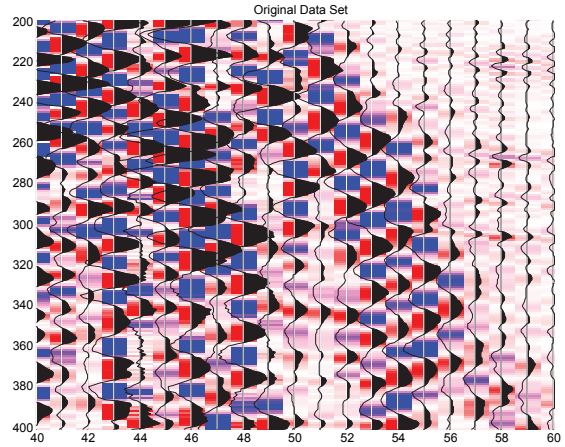

(a)

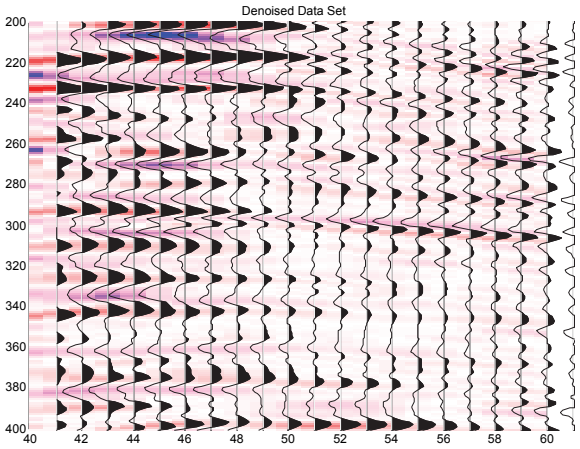

(b)

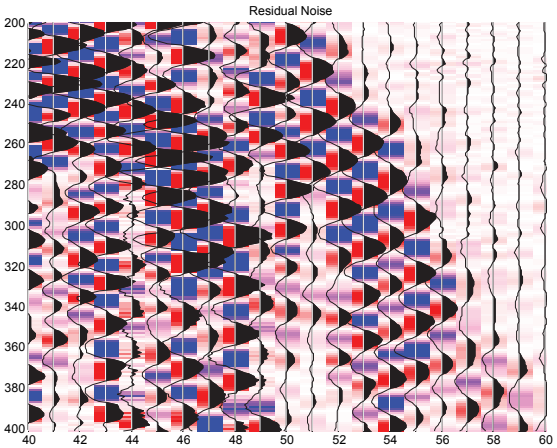

(c)

Figure 5: An area showing the denoising result without the bayesian threshold. We can see the effectiveness of the ground roll removal in this zoomed section more clearly. The wiggle traces have been scaled by image amplitude, color maps scales are constant for all images.